Renewable Energy 119 (2018) 490–503

Contents lists available at ScienceDirect

Renewable Energy

journal homepage: www.elsevier.com/locate/renene

Optimization of autonomous combined heat and power system including PVT, WT, storages, and electric heat utilizing novel evolutionary particle swarm optimization algorithm

A. Lorestani, M.M. Ardehali*

Energy Systems Laboratory, Center of Excellence in Power Systems, Department of Electrical Engineering, Amirkabir University of Technology (Tehran Polytechnic), Tehran, Iran

ARTICLE INFO

Article history:
Available online 22 December 2017

Keywords:
Renewable energy
Combined heat and power
Solar
Wind
Evolutionary particle swarm optimization

ABSTRACT

Renewable energy (RE) sources can be incorporated in design of combined heat and power (CHP) systems, so that the advantages of zero environmental emissions as well as higher energy efficiencies are realized simultaneously. Further, due to inability to dispatch renewable energy sources, the integration of thermal and electricity storages is necessary to enhance the performance of RE-CHP systems in terms of overall cost and reliability to meet thermal and electrical loads. In addition, the utilization of excess electrical energy for conversion to heat could be critical to meeting thermal load and, hence, maintaining the autonomous operation of RE-CHP systems. The goal of this study is to develop a simulation model for optimization of an autonomous RE-CHP system, where thermal and electrical loads are met utilizing photovoltaic (PV)-thermal (PVT) panel, wind turbines (WTs), thermal energy storage, electrical energy storage, and electric heater (EH). For optimization, a newly developed evolutionary particle swarm optimization (E-PSO) algorithm is introduced and validated. It is shown that, as an autonomous RE-CHP system, the combination of PVT, WT, storages, and EH can effectively meet thermal and electrical loads with an acceptable reliability. Moreover, the results confirm the superiority of the proposed E-PSO algorithm among other methods.

1. Introduction

Renewable energy (RE) sources could be integrated to serve autonomous combined heat and power (RE-CHP) systems in remote areas, where the distribution system costs for non-renewable energy carriers are not favorable [1]. However, due to intermittencies in RE sources, reliability concerns prompt for utilization of energy storages in conjunction with RE-CHP systems to meet thermal and electrical time varying loads simultaneously, which in turn necessitates the employment of an energy management strategy (EMS) to ensure that proper energy distribution is achieved.

To identify the contribution of this study, the review of literature with a focus on various aspects of utilization of RE and fuel based sources for meeting thermal and/or electrical loads is summarized in Table 1. In the literature, there are numerous studies that have been conducted for autonomous application of RE sources with storage capabilities for generation of electricity alone [2–11]. There are also studies that have considered application of RE and non-RE sources to simultaneously meet thermal and electrical loads as in CHP systems, however, the optimal design of the examined systems in those studies are based on non-autonomous operation mode and in parallel with the grid [12–19].

Sharafi et al. [20] proposed a multi-objective approach to determine the optimal size of a hybrid renewable energy system for a grid-tied residential energy system, including PV, WT, heat pump, biomass boiler, solar thermal system, and heat storage tank, where it is shown that RE source can play a considerable role in a CHP system. Because photovoltaic-thermal (PVT) panel generates thermal and electrical energy simultaneously, and, in comparison with PV cell and solar thermal system, has higher total efficiency than the sum of the efficiencies of PV cell and solar thermal system, PVT panel can be considered as an effective alternative to supplying thermal and electrical loads on individual basis [21–23]. Furthermore, it has been shown that utilization of thermal energy enhances PVT panel electrical energy production [24]. In a parametric study, the performance of a concentrating PVT CHP system with an attached heat

* Corresponding author.
E-mail address: ardehali@aut.ac.ir (M.M. Ardehali).

https://doi.org/10.1016/j.renene.2017.12.037
0960-1481/

Table 1
Summary of studies on utilization of RE and fuel based sources for autonomous and non-autonomous modes of operation in the literature.

Ref.	RE Source			Fuel Based Sources			Operation Mode	CHP	Storage		Auxiliary Heat	Reliability Analysis	Optimization
	PVT	PV	WT	FC	MT	Diesel Generator			TES	EES			
[2]	–	✓	✓	–	–	–	Autonomous	–	–	✓	–	✓	Iterative Approach
[3]	–	✓	✓	–	–	✓	Autonomous	–	–	✓	–	✓	PSO
[4]	–	✓	✓	✓	–	–	Autonomous	–	–	✓	–	✓	Iterative Approach
[5]	–	✓	✓	–	–	✓	Autonomous	–	–	✓	–	✓	HSA
[6]	–	✓	✓	✓	–	–	Autonomous	–	–	✓	–	✓	GA
[7]	–	✓	✓	✓	–	–	Autonomous	–	–	✓	–	✓	PSO
[8]	–	✓	✓	–	–	✓	Autonomous	–	–	✓	–	–	Iterative Approach
[9]	–	✓	✓	–	–	–	Autonomous	–	–	✓	–	✓	PSO
[10]	–	✓	✓	–	–	–	Autonomous	–	–	✓	–	✓	PSO
[11]	–	✓	✓	–	–	–	Autonomous	–	–	✓	–	✓	CS
[12]	–	–	–	–	✓	✓	Non-Autonomous	✓		✓	NG boiler	–	PSO
[13]	–	–	–	✓	–	✓	Non-Autonomous	✓	–	✓	NG	–	ICA
[14]	–	–	–	✓	–	✓	Non-Autonomous	✓	–	✓	NG	–	HSS
[15]	–	–	–	–	–	✓	Non-Autonomous	✓	✓	–	NG boiler	–	MINP
[16]	–	✓	✓	–	✓	–	Non-Autonomous	✓	✓	–	NG boiler	–	SA
[17]	–	✓	–	✓	–	✓	Non-Autonomous	✓	✓	–	NG boiler	–	LP
[18]	–	✓	✓	✓	✓	–	Non-Autonomous	✓	–	✓	NG boiler	–	QP and PSO
[19]	–	✓	✓	✓	✓	–	Non-Autonomous	✓	–	✓	Biomass boiler	✓	SQP
[20]	–	✓	✓	–	–	–	Non-Autonomous	✓	–	✓	Biomass boilers, Electric Pump	–	PSO
[23]	✓	–	–	–	–	–	Non-Autonomous	✓	✓	–	NG boiler	–	LMM
[26]	✓	–	–	–	–	–	Autonomous	✓	✓	✓	–	–	GA
This Study	✓	✓	✓	N/A	N/A	N/A	Autonomous	✓	✓	✓	EH	✓	Proposed E-PSO

*N/A: Fuel based sources are assumed not available in this study.

storage tank as a thermal energy storage (TES) is investigated and it is found that the efficiency of the concentrating PVT panel decreases when the inlet temperature is increased [25]. For an autonomous RE-CHP application, a feasibility study for utilization of an autonomous PVT CHP system for a residential application is conducted by Gholami et al. [26], where it is shown that utilization of TES and electrical energy storage (EES) is crucial for meeting both thermal and electrical loads and, the capacities of TES and EES greatly affect the reliability and economy of the autonomous system. Further, it is suggested that the auxiliary sources such as connection to the grid and use of natural gas (NG) boiler are necessary for backup. For optimization, genetic algorithm (GA) is used in that study, however, its performance has not been evaluated and compared with other widespread optimization algorithms.

1.1. Contributions

From the review of literature, it is determined that the realization of higher operational efficiency from CHP systems is examined in studies that are limited to the use of fuel-based technologies, such as diesel generator, microturbine (MT), fuel cell (FC) and boilers for non-autonomous applications. For autonomous applications, however, fuel based technologies cannot be utilized as remote areas are rarely provided with NG fuel piping prior to electrification and, it is therefore concluded that autonomous RE-CHP systems for building applications require further investigation from viewpoint of optimal design, economic feasibility, and environmental emissions.

It is anticipated that the combination of PVT and WT could serve as complementary sources for autonomous operation of RE-CHP system and, the integration of the noted RE sources with TES and EES is expected to enhance the performance of RE-CHP system in terms of overall cost and reliability to meet loads. In addition, it is hypothesized that inclusion of an electric heater (EH) could provide for the necessity of meeting thermal loads by converting excess electrical energy to heat. The goal of this study is to develop a simulation model for optimization of an autonomous RE-CHP system, where thermal and electrical loads are met utilizing a PVT panel, WTs, TES, EES and EH. For integrated operation of RE-CHP system, an energy management system (EMS) for managing energy distribution is used so that the total capital and operational and maintenance costs of the autonomous RE-CHP system is minimized. For optimization, a newly developed evolutionary particle swarm optimization (E-PSO) algorithm is introduced and validated.

The remainder of this study is organized as follows. In Section 2, the autonomous RE-CHP system modeling is discussed. Problem formulation and E-PSO optimization algorithm are presented in Sections 3 and 4, respectively. Parametric values used for simulation are given in Section 5. Results and discussions are explained in Section 6 and, Section 7 draws the concluding remarks along with recommended future work. It is noted that all variables are defined in the nomenclature.

2. RE-CHP system modeling

The examined autonomous RE-CHP system is shown in Fig. 1, where PVT panel is employed to generate thermal and electrical energy and WTs are used to complement generation of electricity by PVT panel. As directed by EMS, energy storages may operate in charging or discharging modes to fulfill thermal and electrical loads requirements and, EH is intended to serve as an auxiliary heat source. Based on such configuration, the thermal load can be supplied by PVT, TES or EH, where EH utilizes electrical energy from PVT, WT and/or EES. Also, the electrical load can be supplied by the PVT, WT, or EES.

2.1. Photovoltaic-thermal panel

During day time and as electricity is being generated, the solar irradiation causes temperature increase in PV cells, which has an

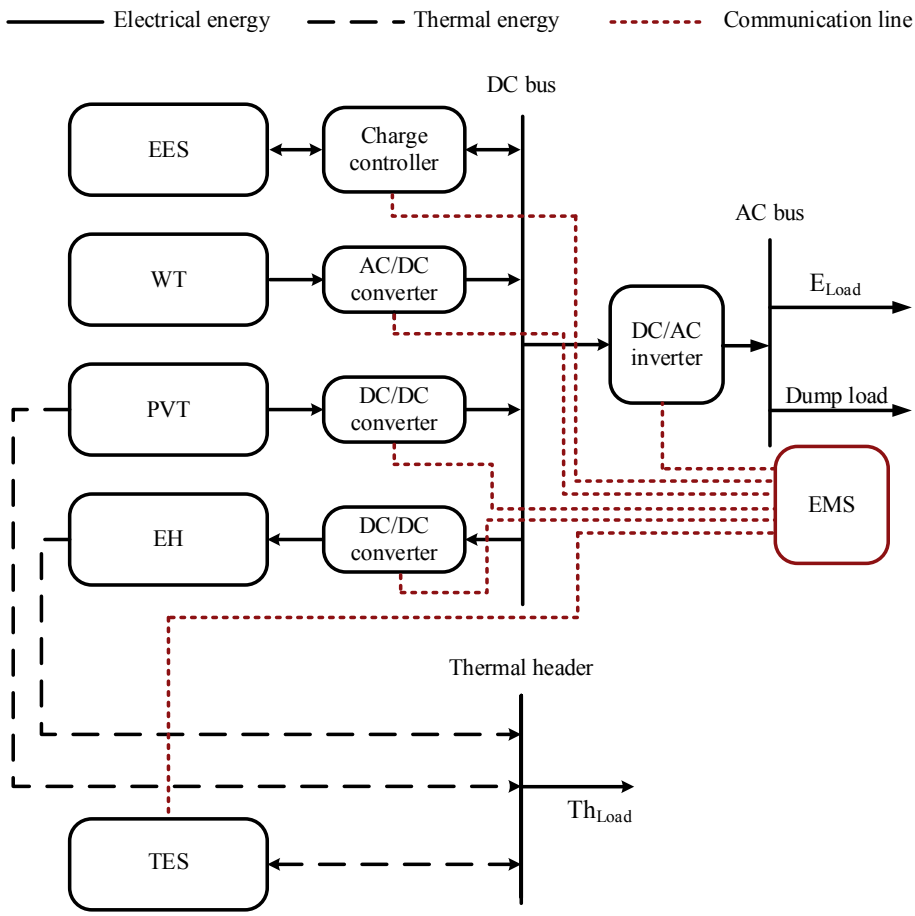

Fig. 1. Autonomous RE-CHP system configuration proposed in this study.

adverse effect on PV electrical efficiency. Appropriate circulation of a working fluid in the underside heat exchanger of PVT panel provides for extracting heat and therefore keeping the electrical generation efficiency at satisfactory levels. The extracted thermal energy maybe used to meet thermal load partially or in full and the excess may also be directed to TES by EMS.

The thermal efficiency of a PVT panel can be calculated as [26].

$$\eta_{th}^{t} = F_R\left[\tau\alpha_{PVT} - \frac{U_{loss}\left(T_f^t - T_a^t\right)}{G^t}\right] \tag{1}$$

and the useful thermal energy generated by PVT panel is given by Ref. [26].

$$Th_{PVT}^{t} = A_{PV}F_R\left[\tau\alpha_{PVT}\cdot G^t - U_{loss}\left(T_f^t - T_a^t\right)\right] \tag{2}$$

where it is assumed that the PVT panel is completely covered with PV cells. The electrical efficiency of the PVT panel depends on the fluid working temperature. The electrical efficiency of PVT panel can be expressed as [26].

$$\eta_E^t = \eta_{ref}\left(1 - \beta_{ref}\left(T_{PM}^t - NOCT\right)\right) \tag{3}$$

where T_{PM} is determined from

$$T_{PM}^t = T_f^t + \left(Th_{PVT}^t(1 - F_R)\right)\Big/(AF_RU_{loss}) \tag{4}$$

It is noted that Eqs. (3) and (4) show the interdependencies of electrical and thermal energy generated by PVT in each hour of operation.

2.2. Wind turbine

The electrical power generation of a WT at time t can be expressed as a function of wind velocity [3].

$$E_{WT}^t = \begin{cases} 0 & V_w^t < V_{w,cut-in} \,||\, V_w^t > V_{w,cut-out} \\ V_w^{t3}\left(\dfrac{E_{WT,r}}{V_{w,r}^3 - V_{w,cut-in}^3}\right) - E_{WT,r}\left(\dfrac{V_{w,cut-in}^3}{V_{w,r}^3 - V_{w,cut-in}^3}\right) & V_{w,cut-in} < V_w^t < V_{w,r} \\ E_{WT,r} & V_{w,r} < V_w^t < V_{w,cut-out} \end{cases} \tag{5}$$

As the wind speed changes with height, the measured wind speed at anemometer height must be converted to desired hub height [27].

$$\frac{V_{w,2}}{V_{w,1}} = \left(\frac{h_2}{h_1}\right)^{\alpha} \tag{6}$$

2.3. Energy storages

To overcome the intermittent nature of renewable sources, two types of energy storages are used to assist with meeting thermal and electrical loads by the RE-CHP system considered in this study.

2.3.1. Thermal energy storage

The energy stored in TES tank at the time t is [15].

$$SOC_{TES}^{t} = SOC_{TES}^{t-1} \times (1-\varepsilon) + \left(Th_{PVT}^{t} - Th_{Load}^{t}/\eta_h\right) \tag{7}$$

$$Th_{TES}^{t} = SOC_{TES}^{t} - SOC_{TES}^{t-1} \tag{8}$$

2.3.2. Electrical energy storage

The capacity of the battery bank as EES is calculated based on number of autonomy days (AD), which implies the number of days a battery bank can provide the load connected to the system without a recharge by the RE sources [3].

$$Cs_{EES} = \frac{En_{Load}\, AD}{DOD\, \eta_{inv}\, \eta_{EES}} \tag{9}$$

and, the charge level of battery bank at the time t can be calculated based on

$$SOC_{EES}^{t} = SOC_{EES}^{t-1} \times (1-\sigma) + \left(E_{PVT}^{t} + E_{WT}{}^{t} - E_{EH}^{t} - E_{Load}^{t}/\eta_{inv}\right) \times \eta_{EES} \tag{10}$$

$$E_{EES}^{t} = SOC_{EES}^{t} - SOC_{EES}^{t-1} \tag{11}$$

2.4. Electrical heater

As the auxiliary heat source for the RE-CHP system, the EH thermal power generation and electricity consumption is modeled using [28].

$$Th_{EH}^{t} = E_{EH}^{t} \times \eta_{EH} \tag{12}$$

2.5. Energy management system

For proper energy conversion, distribution, and storage, EMS is considered an essential part of RE-CHP system as shown in Fig. 2. While it is always necessary to meet thermal load, meeting the electrical load is subject to a pre-specified LPSP reliability index [29] for the autonomous RE-CHP system examined in this study. Accordingly and as directed by EMS, the RE sources and EES are assigned the task of supplying the shortage of thermal energy through EH, if thermal energy produced by PVT and TES is insufficient. The remainder of available electrical energy is assigned to meet electrical load based on a given LPSP.

3. Problem formulation

The optimal design and economics of autonomous RE-CHP system requires that the capacities and quantities of system components are determined, so that the thermal and electrical loads are met and, as a result, the objective cost function is minimized subject to the related constraints.

3.1. Objective cost function

In this study, total annual cost (TAC) [5] is used to form the objective cost function for optimization, which includes initial capital costs as well as operation and maintenance costs,

$$Min\ \{TC_{Cap} + TC_{O\&M}\} \tag{13}$$

where,

$$\begin{aligned} TC_{Cap} = CRF\Big\{ & N_{WT} \times \mathrm{Pr}_{WT} \times E_{WT,r} + A_{PV} \times \mathrm{Pr}_{PVT} \\ & + \mathrm{Pr}_{EES}^{P} \times Cs_{EES} + \mathrm{Pr}_{TES} \times Cs_{TES} + \mathrm{Pr}_{EH} \times E_{EH,r} \\ & + \mathrm{Pr}_{Conv/inv}^{P} \times N_{Conv/Inv} \Big\} \end{aligned} \tag{14}$$

$$TC_{O\&M} = A_{PVT} \times C_{PVT}^{O\&M} + N_{WT} \times E_{WT,r} \times C_{WT}^{O\&M} \tag{15}$$

and note that, there is no cost associated with environmental emission due to utilization of RE-CHP system.

To convert the initial capital cost to annual capital cost, the capital recovery factor *(CRF)* is used [10].

$$CRF = \frac{i(1+i)^n}{(1+i)^n - 1} \tag{16}$$

where n is the life span of RE-CHP system.

For EES and converter/inverter, the lifetime $n'(\leq n)$ is used to determine the single payment present worth factor

$$\mathrm{Pr}_{EES}^{\mathrm{p}} = \mathrm{Pr}_{EES}\left(1 + \sum_{k} \frac{1}{(1+i)^k}\right) \qquad \mathrm{k} = n',\ 2n', \ldots, Kn' \leq \mathrm{n} \tag{17}$$

$$\mathrm{Pr}_{\mathrm{Conv/inv}}^{\mathrm{p}} = \mathrm{Pr}_{\mathrm{Conv/inv}}\left(1 + \sum_{k} \frac{1}{(1+i)^k}\right) \qquad \mathrm{k} = n',\ 2n', \ldots, Kn' \leq \mathrm{n} \tag{18}$$

It is noted that in Eq. (15), the operation and maintenance costs for EH, battery, converters/inverters [5] and storage tank are assumed negligible [15].

3.2. Constraints

The optimization of objective cost function of Eq. (13) for RE-CHP system is subject to several constraints as follows.

3.2.1. Thermal balance

As directed by EMS, the thermal load must be met in every hourly time interval,

$$Th_{Load}^{t} = Th_{PVT}^{t} + Th_{EH}^{t} + Th_{TES}^{t} \tag{19}$$

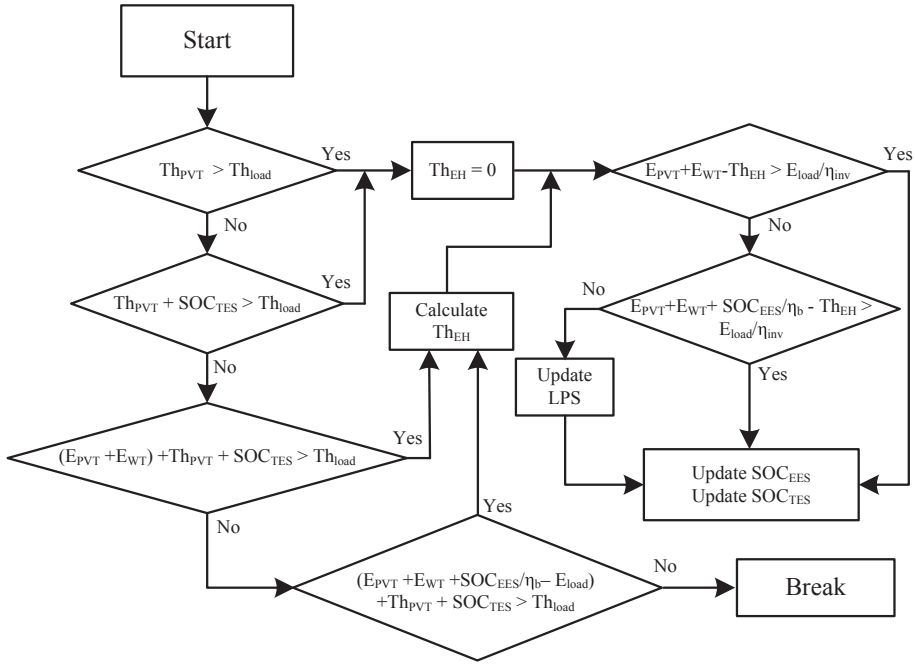

Fig. 2. Flowchart of EMS.

3.2.2. Reliability index for electricity

For optimal design of autonomous RE-CHP systems of this study, reliability is expressed in terms of LPSP, where a value of zero defines a completely reliable system and one indicates that the electrical load is never met. For a specified period, τ (=8760 h in this study), the LPSP index is calculated based on

$$LPSP = \frac{\sum_{t=1}^{\tau} LPS(t)}{\sum_{t=1}^{\tau} E_{Load}(t)} \tag{20}$$

where LPS is the loss of power supply when the available hourly electrical energy is less than electrical load. For design purposes, the following inequality constraint must be observed:

$$LPSP \leq LPSP_{\max} \tag{21}$$

where $LPSP_{\max}$ is specified as the upper bound of LPSP.

3.2.3. Storages

For storages, the following constraints for SOC_{TES} and SOC_{EES} must be satisfied in each hourly time interval

$$SOC_{TES}^{Min} \leq SOC_{TES}^{t} \leq Cs_{TES} \tag{22}$$

$$SOC_{EES}^{Min} \leq SOC_{EES}^{t} \leq Cs_{EES} \tag{23}$$

$$\mathrm{SOC}_{\mathrm{EES}}^{\mathrm{Min}} = (1 - \mathrm{DOD}) \times Cs_{EES} \tag{24}$$

Further, note that in each hourly time step, storage devices cannot charge and discharge, simultaneously.

3.2.4. Limits of optimization variables

The optimization variables (OV) include $A_{PV}N_{WT}$, AD, Cs_{TES} and $E_{EH,r}$ which must be determined through each iteration of the optimization procedure and must be within the allowable limits based on

$$OV = \begin{cases} OV^{Min} & if \;\; OV < OV^{Min} \\ OV^{Max} & if \;\; OV > OV^{Max} \\ OV & otherwise \end{cases} \tag{25}$$

4. Optimization

The optimal design and economics of autonomous RE-CHP system subject to the noted constraints is a nonlinear, non-smooth, and non-convex problem that is solved based on E-PSO algorithm that benefits from several enhancements developed in this study for implementation in PSO algorithm, as described in this section.

4.1. Particle swarm optimization algorithm

The PSO algorithm is based on the sociality of bird flocks looking for food [12,30], where velocity and position of each bird, identified as particle, is determined in each iteration. It is assumed that there are $nPop$ particles in the DM dimensional search space. For each particle j in each iteration it, the position, personal best position, and corresponding fitness value are X_j^{it}, $Pbest_j^{it}$ and $f_{X,j}(\mathrm{j} = 1, 2, \ldots, nPop)$, respectively. The best location of the swarm is $Gbest$ and the corresponding fitness value is $fGbest$ and, the velocity of particle j is V_j. The position and velocity of particle j in each iteration are updated based on

$$\begin{cases} V_j^{it+1} = C\left(\omega V_j^{it} + C_1 \cdot Rand_1().\left(Pbest_j^{it} - X_j^{it}\right) + C_2 \cdot Rand_2()\cdot\left(Gbest - X_j^{it}\right)\right) \\ X_j^{it+1} = X_j^{it} + V_j^{it+1} \end{cases} \tag{26}$$

where ω, C_1 and C_2 are inertia, cognitive, and social weights, respectively. Also, $Rand_1$ and $Rand_2$ are the uniform distributed random numbers in the range of [0, 1]. Further, for displacement range of each particle, the following relation is applied after updating velocity,

$$V_j^{it+1} = \begin{cases} V_j^{it+1,Min} & if\ V_j^{it+1} < V_j^{it+1,Min} \\ V_j^{it+1,Max} & if\ V_j^{it+1} > V_j^{it+1,Max} \\ V_j^{it+1} & otherwise \end{cases} \tag{27}$$

4.2. Proposed evolutionary particle swarm optimization

Although PSO is a powerful algorithm with high speed convergence, the main disadvantage is getting trapped in a local optimum solution because of loss of diversity of swarm [31]. In this study, PSO algorithm is enhanced using three operators adapted from differential evolution (DE) algorithm for escaping from possible local optimum solution and additional computational efficiency. In addition, it is expected that proper tuning of E-PSO parameters would improve the exploitation and exploration of the algorithm. In the proposed E-PSO algorithm, the three main coefficients that strongly affect the performance of the algorithm are dynamically updated using arc-tangent based relations as described later in this section.

4.2.1. Mutation operation

The E-PSO algorithm employs the mutation operation which produces a mutant vector M_j with respect to each individualX_j, referred to as target vector, in the current population. For target vector X_j in each iteration, the associated mutant vector can be generated based on

$$M_j^{it} = X_{r_1^j}^{it} + F \cdot \left(X_{r_2^j}^{it} - X_{r_3^j}^{it}\right) \quad j = 1, 2, \ldots, nPop \tag{28}$$

where indices r_1^j, r_2^j and $r_3^j$are mutually exclusive integers generated randomly within [1,$nPop$]. The scaling factor F is a random positive parameter within$[F^{Min}, F^{Max}]$.

4.2.2. Crossover operation

After the mutation operation step, the crossover operation is applied to each pair of the target vector $X_j = (x_j, x_j \ldots x_j)$ and its corresponding mutant vector $M_j = (m_j, m_j \ldots \mathrm{m}_j)$ to generate a trial vector$T_j = (t_j, t_j \ldots t_j)$. The crossover operation used in E-PSO algorithm is defined as

$$t_j^b = \begin{cases} m_j^b & if\ (rand_b[0,1) \le CR)\ or\ (\mathrm{b} = \mathrm{b}_{rand}) \\ x_{j,k}^b & otherwise \\ \mathrm{b} = 1, 2, \ldots, DM \end{cases} \tag{29}$$

where crossover rate CR is a user-specified constant within the range [0,1), and controls the fraction of parameter values copied from the mutant vector. The parameter $b_{rand}$is a randomly chosen integer in the range of $[1, DM]$. The applied crossover operator copies the bth parameter of the mutant vector $M_j^{it}$to the corresponding element in the trial vector T_j if $(rand_b[o, 1) \le CR)$ or $b = b_{rand}$, otherwise, it is copied from the corresponding target vectorX_j.

4.2.3. Selection operation

The selection operator chooses the vectors that compose the population in the next iteration. This operator compares the fitness of the trial vector and the corresponding target vector and selects the one that leads to better solution. Then, out of the two vectors, the one that is more fit is allowed to enter the next step.

4.2.4. Dynamic update of parameters

As noted earlier, the three parameters that strongly affect the performance of E-PSO algorithm are inertia weight, cognitive weight, and social weight coefficients [9]. A large value for ω results in better global searching capability, while a small value for ω makes the algorithm more suitable for local search. Therefore, dynamic adjustment of ω enhances the performance of E-PSO algorithm. At the beginning of a search, a large ω contributes to mutation for more effective exploration and at the later iterations, the exploitation can be greatly enhanced by small inertia weight. The cognitive weight C_1 signifies the affection of personal best experience and, at the start of the search, C_1 should be large to enhance the exploration. However, during the final iterations, C_1 is better to be small to improve exploitation [10]. For the social weight C_2, at the start of the search, it should have little influence on the particle position, whereas, during the final iterations, it should be large to enhance the social communication between particle swarm. For implementing the E-PSO algorithm, the three noted coefficients are dynamically adjusted at each iteration based on

$$\omega(it) = 0.5 \times \left(\omega^{Max} + \omega^{Min}\right) + K_\omega \times \left[\arctan\left(\frac{-2\pi}{MaxIt} \times it + \pi\right)\right] \times \left(\omega^{Max} - \omega^{Min}\right) \tag{30}$$

$$C_1(it) = 0.5 \times \left({C_1}^{\max} + {C_1}^{\min}\right) + K_{C_1} \times \left[\arctan\left(\frac{-2\pi}{MaxIt} \times it + \pi\right)\right] \times \left({C_1}^{\max} - {C_1}^{\min}\right) \tag{31}$$

$$C_2(it) = 0.5 \times (C_2 + C_2) + K_{C_2} \times \left[\arctan\left(\frac{2\pi}{MaxIt} \times it - \pi\right)\right] \times (C_2 - C_2) \tag{32}$$

Based on the flowchart of simulation procedure shown in Fig. 3, the process starts with generating the parent vector for E-PSO algorithm. After the primary loop, operators of mutation and crossover are applied to create the trial vector. Comparing the fitness values, the parent vector is obtained and the personal and global best of each particle are updated. This procedure is repeated for all population and then all parent vectors are determined. Then, the

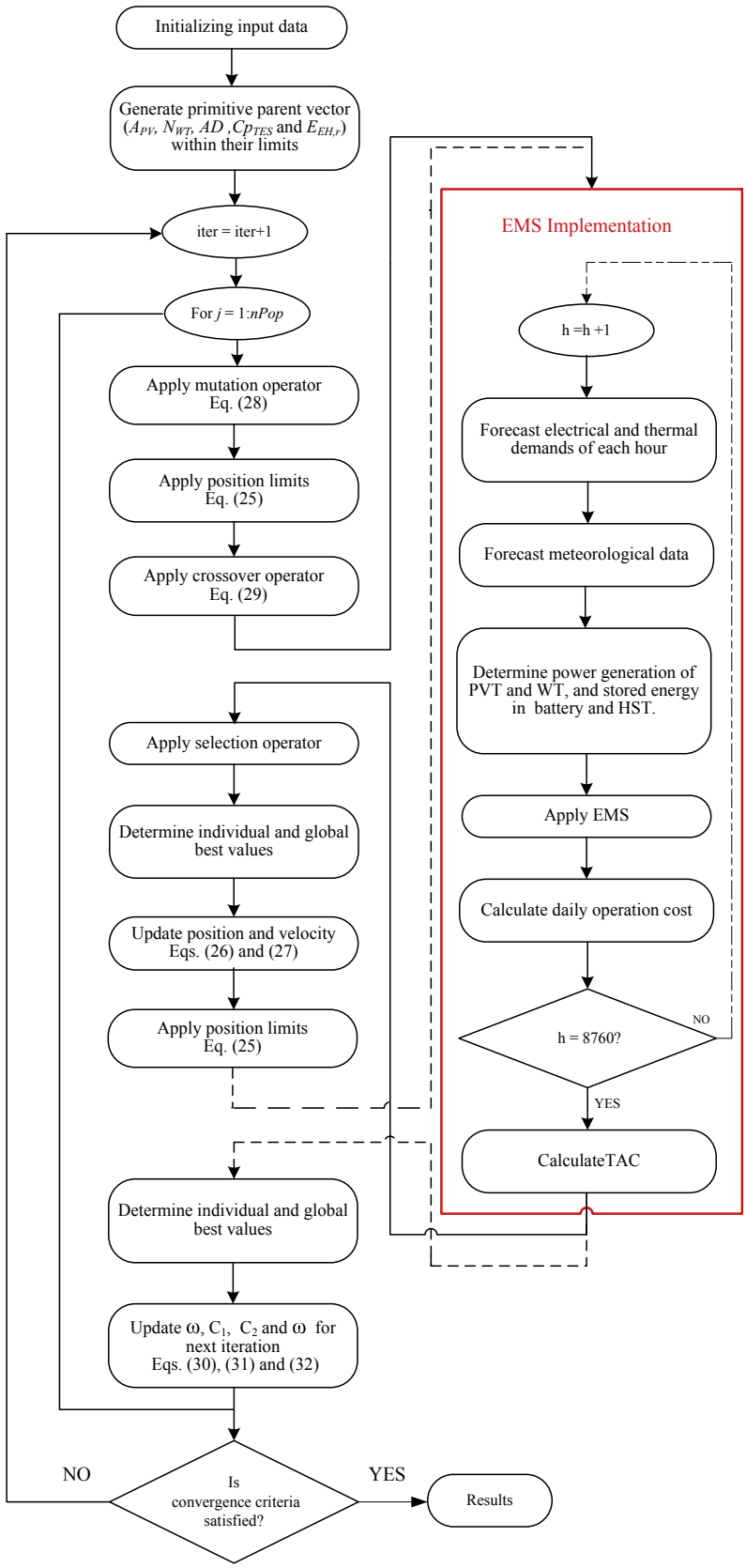

Fig. 3. Flowchart of simulation procedure for E-PSO algorithm developed in this study.

position and velocity of particles in parent vector are updated according to the PSO rules to produce another set of solutions and, the global and personal best values are also determined for the next iteration.

5. Parametric values

The hourly meteorological data for wind speed, insolation, and air temperature used for simulation are for Rafsanjan, Iran (30.40 N latitude; 55.99 E longitude) [3] shown in Fig. 4. The simulation is conducted for 8760 h and the useful life of the RE-CHP system is 24 years. For simulation purposes over 24 years of planning horizon, the hourly electricity and thermal loads are for mid-season day of each season [16]. The 24 h load of mid-season day represents the daily loads of an entire season. While the mid-season daily load is constant for an entire season, the meteorological data used are for 8760 h of the year and, it is assumed that the yearly load and meteorological data remain constant over the operation horizon [3–6,10]. It is noted that the maximum electrical load is 42 kW in summer and the maximum heating load is 80 kW in winter for a remotely located office building equipped with autonomous RE-CHP system.

The components specifications of autonomous RE-CHP system are given in Table 2. The capital and operation and maintenances costs of storage tank and EH are assumed negligible [12,15]. Also, it is assumed that TES and EES are initially empty and, $LPSP_{max}$ is set to 0.02 [7].

The number of design variables for simulation of RE-CHP is equal to 5 which constitutes the dimension of each particle in E-PSO algorithm as noted in Eq. (22). The simulation parameters for E-PSO algorithm are provided in Table 3. For Eqs. 30–32, the variations of inertia, cognitive, and social weights, during 200 iteration of E-PSO algorithm developed in this study are shown in Fig. 5.

6. Results and discussion

6.1. Validation of optimization algorithm

To validate the performance and effectiveness of the proposed E-PSO algorithm, the simulation of RE-CHP system has been performed for 30 independent runs and, the results of E-PSO algorithm are compared to those of other algorithms including DE, PSO, GA, and HSA, as listed in Table 4. It is observed that the values for minimum, maximum, and average TAC of RE-CHP system for E-PSO during 30 different runs are close to each other, which demonstrates the effectiveness of the enhancements introduced in E-PSO algorithm in this study. In addition, the best, average and worst values of the objective cost functions obtained by E-PSO are better than the corresponding results from all the noted algorithms. Also, it is found that the average of results of the proposed E-PSO algorithm is better than the best results from other algorithms. Based on 30 independent runs, the standard deviation of the proposed E-PSO is $3.21, which is considerably lower than those of other algorithms. For simulation time, the results show that the proposed E-PSO algorithm performs more favorably. While the execution of three operators and three dynamic coefficient tuning equations may seem to be more time consuming in advance, the E-PSO algorithm requires less simulation time to achieve better results with lower number of initial population. As shown in Table 4, the initial population of E-PSO is 18; however, this parameter for other algorithms is higher for achieving proper convergence (Fig. 6). Hence, it is determined that the proposed E-PSO algorithm, as compared with other optimization methods, can search the feasible space more effectively and reach the global optimum with lower number of cost function evaluation.

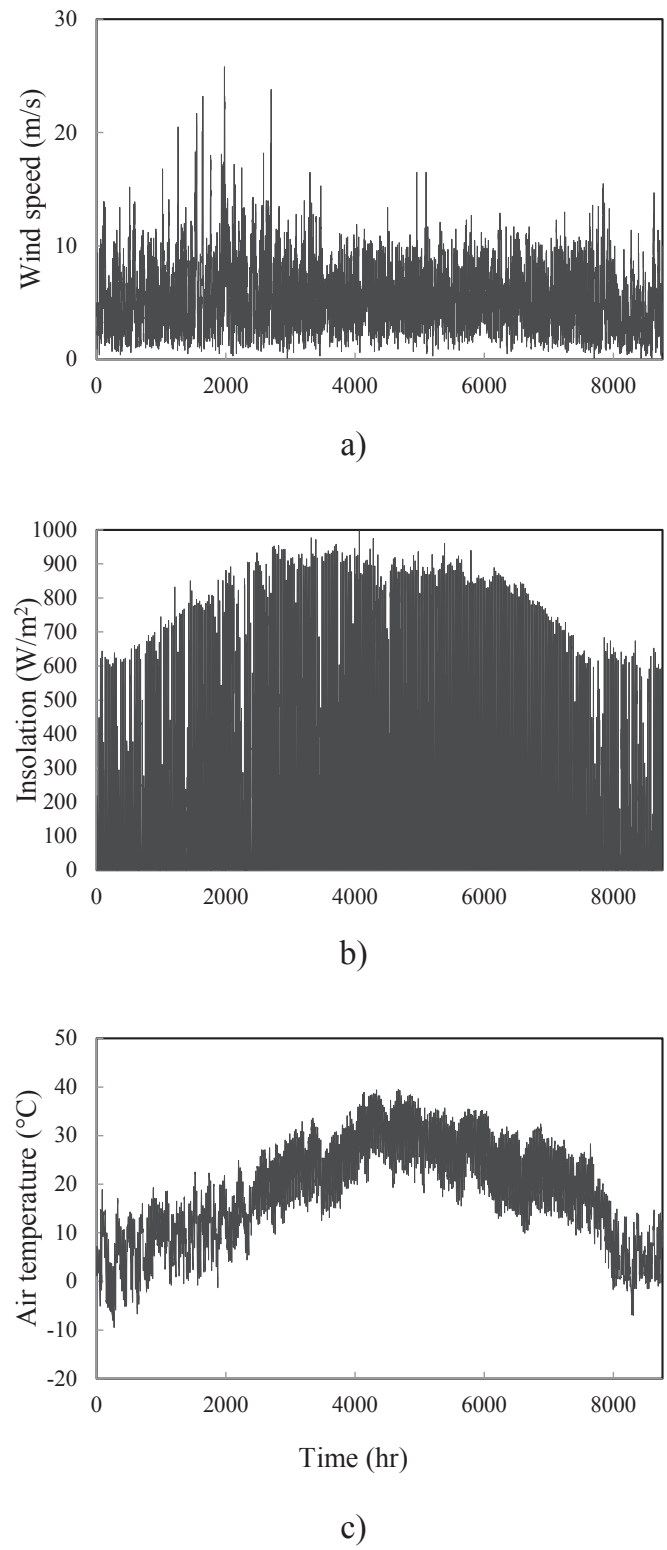

Fig. 4. Hourly profile of meteorological data during a year: a) wind speed (at height of 10 m), b) insolation, and c) air temperature [3].

The sensitivity of simulation results to the proposed enhancements of the E-PSO algorithm for 30 independent runs is shown in Table 5, where the impacts of tuning the proposed dynamic parameters and the exclusion of mutation, crossover, and selection operators on exploration and exploitation of the algorithm are

Table 2
RE-CHP components specifications [3–5,15,26,28].

Parameter	Value (Unit)
PVT	
Pr_{PVT}	415.4 ($/m^2)
$C_{PVT}^{O\&M}$	2 (%)
n'	24 (years)
η_{ref}	0.15
β_{ref}	0.005
$\tau\alpha_{PV}$	0.75
U_{loss}	7 (W/m^{2}K)
F_R	0.85
$NOCT$	297 (K)
WT	
$V_{w,cut-in}$	2.5 (m/s)
$V_{w,r}$	9.5 (m/s)
$E_{WT,r}$	10 (kW)
Pr_{WT}	2700 ($/kW)
$C_{WT}^{O\&M}$	2 (%)
Voltage	48 (V)
α	0.14
n'	25 (years)
EES	
η_{EES}	85 (%)
n'	5 (years)
Pr_{EES}	280 ($/kWh)
DOD	80 (%)
σ	0.0002
TES	
Pr_{TES}	0
η_h	0.9
ε	0.05
EH	
η_{EH}	0.98
Pr_{EH}	40 ($/kW)
Inverter/Converter	
η_{inv}	0.95
n'	10 (years)
$Pr_{Conv/inv}$	2000 ($)

Table 3
E-PSO algorithm simulation parameters used in this study.

Parameter	Value
DM	5
$nPop$	18
$MaxIt$	200
ω^{Max}	1
ω^{Min}	0.4
k_ω	0.4
C_1^{Max}	1.5
C_1^{Min}	0.1
k_{C_1}	0.4
C_2^{Max}	1.5
C_2^{Min}	0.1
k_{C_2}	0.4
F^{Max}	0.2
F^{Max}	0.7
CR	0.4

determined. It is found that the exclusion of the noted operators results in higher average TAC. This trend is also observed for C_1, C_2 and ω non-linear tuning.

6.2. RE-CHP operational performance

The optimal values for design parameters of RE-CHP system and the corresponding TAC and LPSP based on E-PSO algorithm are shown in Table 6. The calculated TAC of the system is $56310.98 and, it is observed that LPSP for the autonomous RE-CHP system is 0.01which is less than $LPSP_{max}$ of 0.02, while thermal load is met in full in every hour of the year.

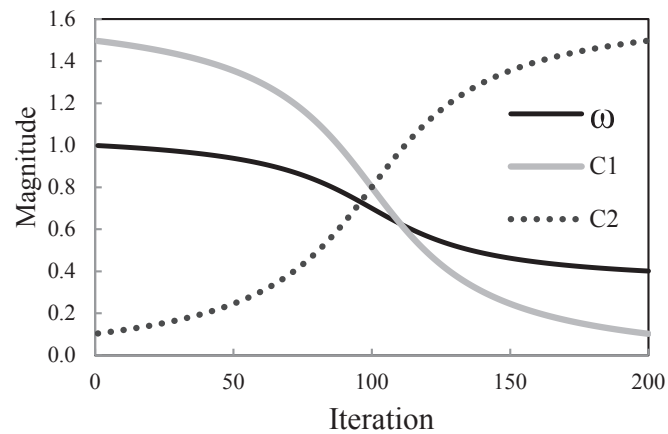

Fig. 5. Variation of inertia, cognitive and social weight coefficients during 200 iterations of E-PSO algorithm developed in this study.

In the optimal design of RE-CHP autonomous system, there exists a tradeoff between costs and reliability and, the sensitivity of TAC to variation in $LPSP_{max}$ is shown in Fig. 7.

The daily thermal and electrical efficiencies of PVT panel during mid-season weak of winter and summer are shown in Fig. 8, where the thermal efficiency based on Eq. (1) reaches 55% in winter and 40% in summer and, the electrical efficiency based on Eq. (3) approaches 14% in winter and 12.5% in summer. As a result, the overall efficiencies of 69 and 52.5% are achieved for PVT panel for winter and summer, respectively. The electrical and thermal performances of RE-CHP for four sample days are depicted in Fig. 9. In general, it is observed that integration of RE sources has resulted in electricity generation by PVT panel and WTs to reduce the effects of inherent intermittencies. For mid-season days for every season, in the early hours of day, while there is no contribution from PVT panel, the electricity generation by WTs and EES meets the electricity base load for the office building and the excess energy is stored in EES. For winter, EH is also activated during the early hours of winter mid-season day and EH consumes electricity to assist with meeting thermal loads. It is also observed that the high thermal efficiency of PVT has resulted in thermal energy generation above and beyond the loads for every season to allow for storage by TES.

6.3. Effects of different configurations

It is of interest to examine the effects of different configurations of RE sources on TAC of the RE-CHP system. The importance of utilizing solar and wind energy sources together in a RE-CHP system is demonstrated in Table 7. It is founded that the TAC of RE-CHP system without PVT has increased by 75%. When PV is used instead of PVT, the TAC of RE-CHP has experienced an increase by more than 55% which indicates that using PVT in RE-CHP system is economically more favorable than using PV. Further, utilization of PVT panel in the autonomous RE-CHP system results in more reliable operation ($LPSP = 0.01$) than RE-CHP system without PVT (WT-TES-EES-EH) or with PV (PV-WT-TES-EES-EH). Also, TAC of RE-CHP system without WT (PVT-TES-EES-EH) has increased by 22.6%. In the absence of WT, the size of PVT has greatly increased and, in the absence of PVT, the number of WTs in PV-WT-TES-EES-EH and PVT-WT-TES-EES-EH systems has increased from 5 to 10 and15, respectively. Further and as to be expected, the absence of WT in

Table 4
Results: Validation of E-PSO algorithm based on TAC values for optimization of autonomous RE-CHP system out of 30 independent runs.

Optimization algorithm	Initial population	Lowest TAC ($)	Average TAC ($)	Highest TAC ($)	Median TAC ($)	Standard deviation	Simulation time (s)
DE	35	56338.60	56480.90	57100.14	56374.95	301.10	358
PSO	50	56462.14	56878.77	57744.56	56776.69	323.54	376
GA	75	56338.61	57044.00	63377.25	56366.21	2103.90	751
HSA	50	56338.61	59731.11	63416.32	56450.04	3585.25	340
E-PSO	18	56310.98	56312.53	56330.06	56310.98	3.21	338

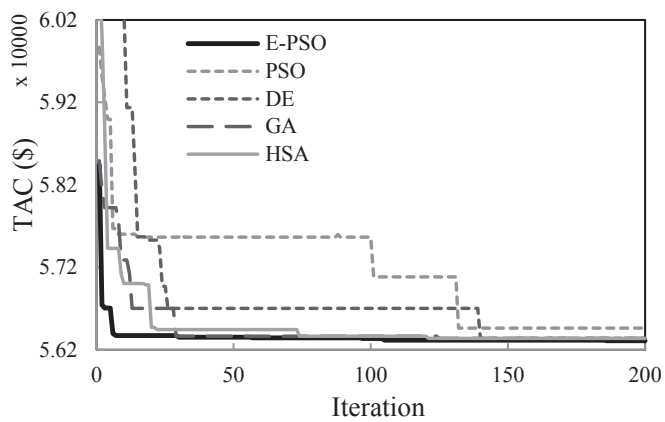

Fig. 6. Validation and convergence comparison of E-PSO with those of PSO, DE, GA and HSA algorithms for the optimization of autonomous RE- CHP system examined in this study.

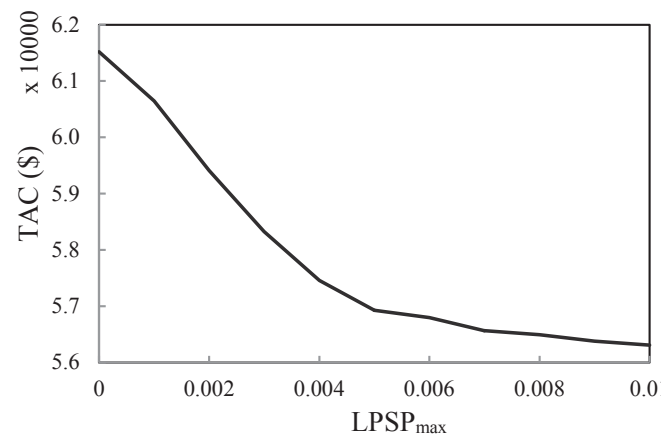

Fig. 7. Effects of reliability level on TAC of the RE-CHP.

Table 5
Results: Sensitivity of TAC results to E-PSO algorithm enhancements for the autonomous RE-CHP system based on 30 independent runs.

Optimization algorithm	Lowest TAC ($)	Average TAC ($)	Highest TAC ($)
PSO	56462.14	56878.77	57744.56
E-PSO without mutation and crossover operators	56314.83	56336.50	56413.58
E-PSO without C_1,C_2 andωnon-linear equation	56313.87	56406.16	56589.80
E-PSO	56310.98	56312.53	56330.06

Table 6
Results: Optimal values for design parameters of autonomous RE-CHP system and the corresponding TAC and LPSP.

Parameters	Lower bound	Optimal values	Upper bound
A_{PV} (m^2)	0	530	2500
N_{WT}	0	5	15
AD	0	0.5	3
$Cs_{EES}(kWh)$		238	
Cs_{TES} (kWh)	0	700	3000
$E_{EH,r}$	0	48	90
$LPSP$	0	0.01	0.02
TAC ($)		56310.98	

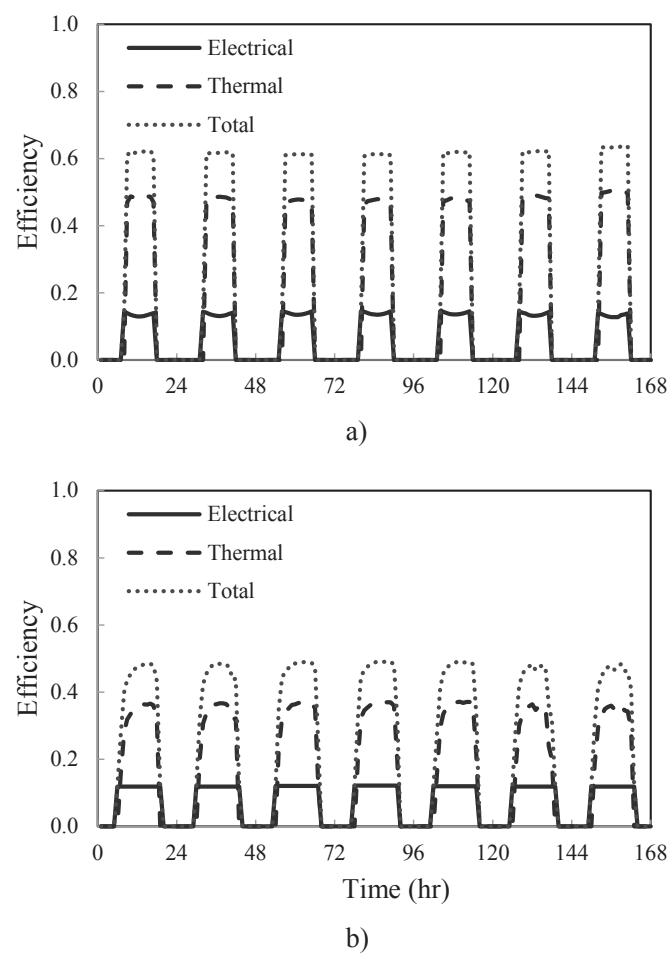

Fig. 8. PVT daily electrical and thermal efficiencies during mid-season weak of a) winter, b) summer.

RE-CHP system results in substantial increase in storage capacities. Without utilization of EH, the TAC of RE-CHP system increases up to $100123.28 and the optimum number of WTs approaches zero, as the conversion of electricity to thermal energy is unavailable.

6.4. Effects of storage sizes

To study the impacts of storage sizes on TAC of the RE-CHP system, sensitivity analyses have been conducted based on *AD* of EES and capacity of TES as shown in Fig. 10. For EES, it is determined

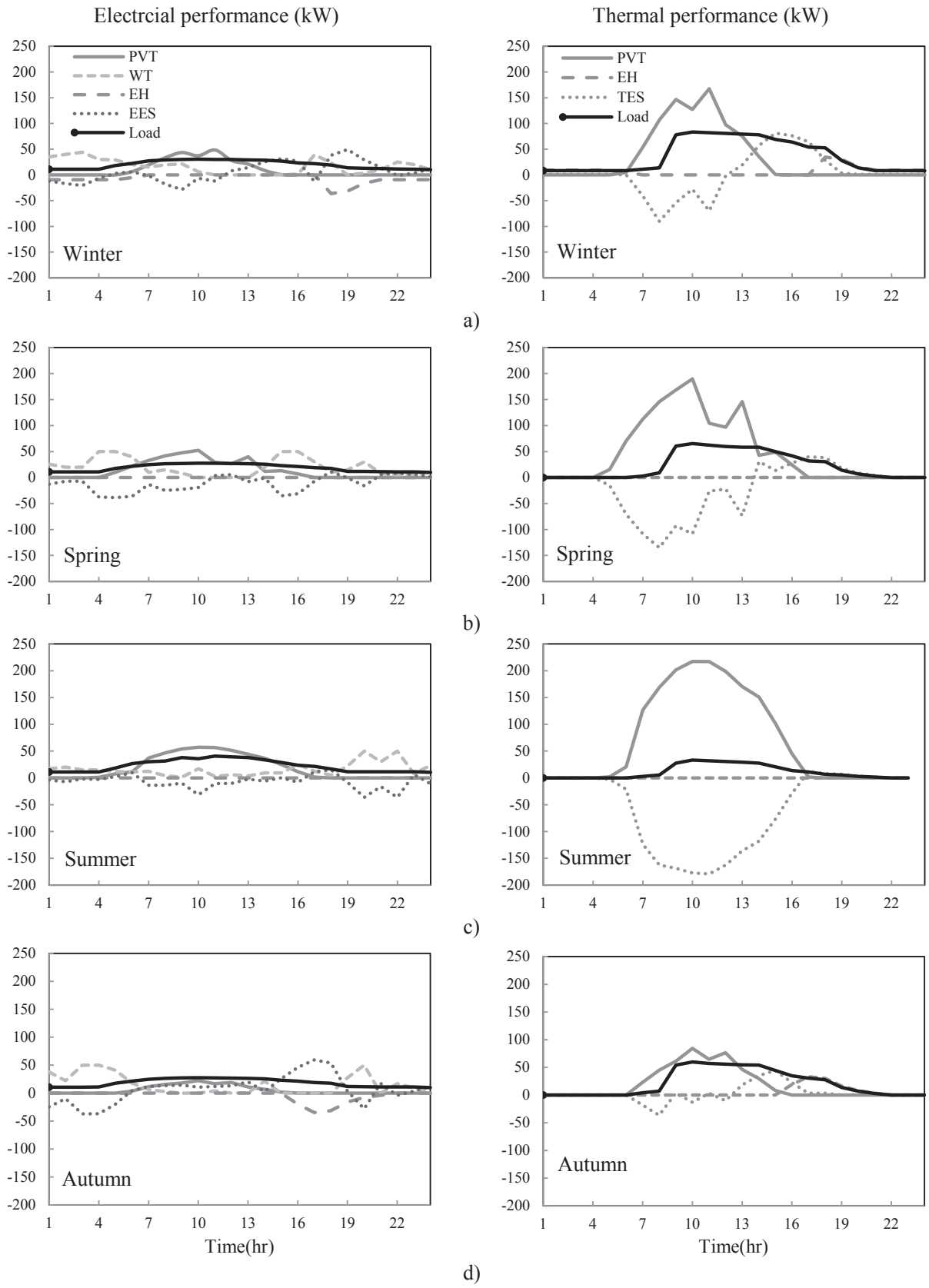

Fig. 9. Results: RE-CHP system operational performance during mid-season day of each season. Note that for storages, (−) value indicates charging and (+) value indicates discharging. For EH, (−) indicates electrical energy consumption and (+) indicates thermal energy production.

Table 7
Results: Comparison of performance for different RE-CHP system configuration.

RE-CHP system configuration	A_{PV} (m^2)	N_{WT}	AD	Cs_{TES}(kWh)	$E_{EH,r}$ (kW)	TAC ($)	LPSP	TAC increase (%)
PVT-WT-EES-TES-EH	530	5	0.5	700	48	56310.98	0.01	–
PV-WT-EES-EH	920	9	2.7	–	90	94478.62	0.02	67.78
WT-EES-EH	–	15	2.77	–	90	102490.32	0.02	82.00
PVT-EES-TES-EH	1155	–	1.42	1650	18	80360.99	0.02	42.71
PVT-WT-EES-TES	2000	0	0.7	1300	–	100123.28	0.02	77.80

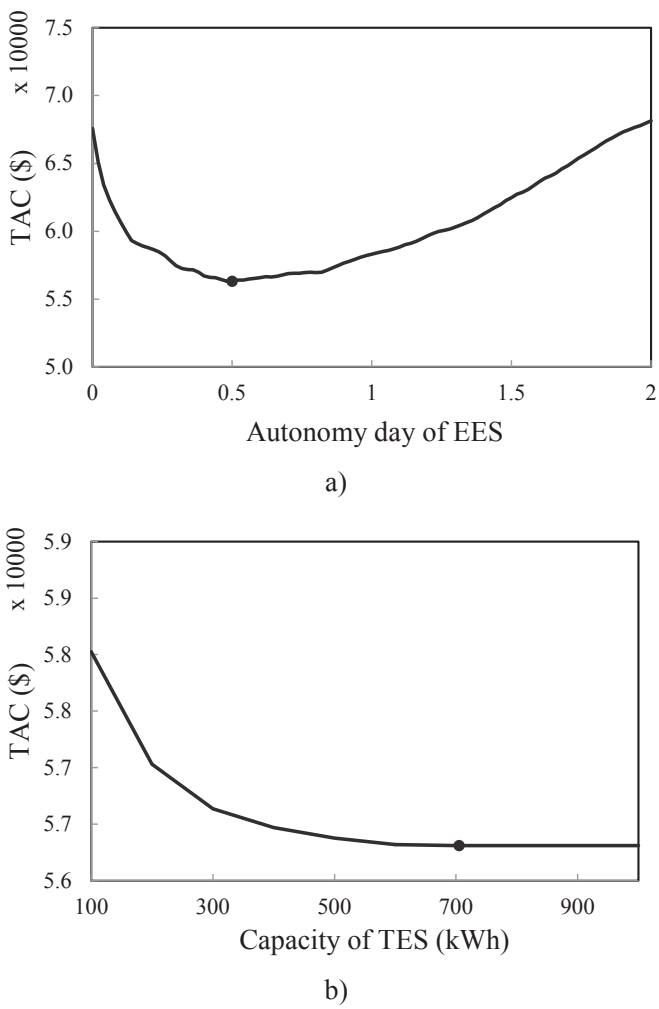

Fig. 10. Effects of RE-CHP system storage sizes on TAC: a) EES, b) TES.

that the minimum TAC occurs at $AD = 0.5$. For TES with zero operation and maintenance cost, the minimum TAC is 700 kWh. It is observed that TAC of RE-CHP system experiences an increasing trend for all values for AD greater or less than $AD = 0.5$, as EES must supply both the electrical load and the thermal load through EH. However, for TES, TAC asymptotically approaches a constant value for TES capacities greater than the optimal value.

6.5. Environmental effects

The air pollution and greenhouse gas emissions due to fossil fuel consumption include NO_x, SO_2, CO and CO_2 and [32], the utilization of RE-CHP is expected to prevent the emission of all such pollutants. For analyzing the environmental effect of the autonomous RE-CHP system, the electrical and thermal energy are examined separately.

Table 8
Results: Annual environmental emission reduction of RE-CHP system.

Generation type		Pollutant			
		NOx	SO2	CO	CO2
Electricity (steam power plant)	Value (g/kWh)	2.68	5.70	1.61	762.04
	Reduction (kg/year)	442.04	940.15	265.55	125689.83
Heating (NG)	Value (g/kWh)	1.33	0.22	0.05	0.36
	Reduction (kg/year)	257.24	42.07	9.55	70.40
Autonomous RE-CHP		0	0	0	0
Total reduction of pollutants		699.28	982.22	275.10	125760.23

The annual environmental emission reductions resulting from utilization of RE-CHP system in terms of equivalent electricity generation and heat production by means of steam power plants and NG, respectively, are given in Table 8, where transmission line and distribution system losses are not accounted for. It is expected that accounting for such losses is dependent on network topologies and would result in higher emissions.

7. Conclusions and recommendations

In this study, the optimal design and economics of autonomous RE-CHP system including PVT, WT, EES, TES and EH for a remotely located office building are examined. An EMS for proper energy distribution is used and, the economic benefits of utilizing the proposed configuration of RE-CHP system are analyzed. The findings confirm that RE sources can be incorporated successfully into the design of CHP systems operated autonomously, when the complementary performances of PVT and WT coupled with storages and EH can provide for meeting thermal and electrical loads throughout the year.

Based on examination of various configuration for RE-CHP systems, the simulation results show that TAC substantially increases, when thermal energy from PV and TES are not utilized (PV-WT-EES-EH). When WT or EH are not included in the RE-CHP configuration, similar increase in TAC can also be expected. For storages, optimal sizing of EES is found to be critical to minimizing TAC. It is concluded that, as the most immediate effect of utilization RE-CHP system for meeting thermal and electrical loads, there exist opportunities for diminishing all environmental pollutants that may otherwise be emitted from use of fossil fuel.

For optimization, the novelty of the newly developed E-PSO algorithm introduced in this study is demonstrated by comparing its performance in terms of convergence and simulation time with those of DE, PSO, GA, and HSA algorithms.

The results of this study confirm that properly designed and configured RE-CHP systems can provide for meeting thermal and electrical loads for remote areas applications with an adequate level of reliability, where the expansion of NG fuel piping and electricity networks may not be economically feasible.

For future work, due to availability of thermal energy from PVT and EH, absorption cooling chiller could be added to system architecture for meeting cooling loads.

References

[1] W. Elsner, M. Wysocki, P. Niegodajew, R. Borecki, Experimental and economic study of small-scale CHP installation equipped with downdraft gasifier and internal combustion engine, Appl. Energy 202 (2017) 213–227, https://doi.org/10.1016/J.APENERGY.2017.05.148.

[2] B.S. Borowy, Z.M. Salameh, Methodology for optimally sizing the combination of a battery bank and PV array in a Wind/PV hybrid system, IEEE Trans. Energy Convers. 11 (1996) 367–373, https://doi.org/10.1109/60.507648.

[3] H. Borhanazad, S. Mekhilef, V. Gounder Ganapathy, M. Modiri-Delshad, A. Mirtaheri, Optimization of micro-grid system using MOPSO, Renew. Energy 71 (2014) 295–306, https://doi.org/10.1016/j.renene.2014.05.006.

[4] R. Hosseinalizadeh, G.H. Shakouri, M.S. Amalnick, P. Taghipour, Economic sizing of a hybrid (PV-WT-FC) renewable energy system (HRES) for stand-alone usages by an optimization-simulation model: case study of Iran, Renew. Sustain. Energy Rev. 54 (2016) 139–150, https://doi.org/10.1016/j.rser.2015.09.046.

[5] A. Maleki, A. Askarzadeh, Optimal sizing of a PV/wind/diesel system with battery storage for electrification to an off-grid remote region: a case study of Rafsanjan, Iran, Sustain. Energy Technol. Assess. 7 (2014) 147–153, https://doi.org/10.1016/j.seta.2014.04.005.

[6] A. Maleki, A. Askarzadeh, Artificial bee swarm optimization for optimum sizing of a stand-alone PV/WT/FC hybrid system considering LPSP concept, Sol. Energy 107 (2014) 227–235, https://doi.org/10.1016/j.solener.2014.05.016.

[7] M.H. Athari, M.M. Ardehali, Operational performance of energy storage as function of electricity prices for on-grid hybrid renewable energy system by optimized fuzzy logic controller, Renew. Energy 85 (2016) 890–902, https://doi.org/10.1016/j.renene.2015.07.05.

[8] F.A. Bhuiyan, A. Yazdani, S.L. Primak, Modeling, simulation, and performance analysis of power management strategies for an islanded microgrid, Int. J. Energy Sci. 3 (2013) 383–394, https://doi.org/10.14355/ijes.2013.0306.02.

[9] A. Askarzadeh, L. dos Santos Coelho, A novel framework for optimization of a grid independent hybrid renewable energy system: a case study of Iran, Sol. Energy 112 (2015) 383–396, https://doi.org/10.1016/j.solener.2014.12.013.

[10] A. Maleki, M. Ameri, F. Keynia, Scrutiny of multifarious particle swarm optimization for finding the optimal size of a PV/wind/battery hybrid system, Renew. Energy 80 (2015) 552–563, https://doi.org/10.1016/j.renene.2015.02.045.

[11] S. Sanajaoba, E. Fernandez, Maiden application of Cuckoo Search algorithm for optimal sizing of a remote hybrid renewable energy System, Renew. Energy 96 (2016) 1–10, https://doi.org/10.1016/J.RENENE.2016.04.069.

[12] H.R. Sadeghian, M.M. Ardehali, A novel approach for optimal economic dispatch scheduling of integrated combined heat and power systems for maximum economic profit and minimum environmental emissions based on Benders decomposition, Energy 102 (2016) 10–23, https://doi.org/10.1016/j.energy.2016.02.044.

[13] H. Karami, M.J. Sanjari, S.H. Hosseinian, G.B. Gharehpetian, An optimal dispatch algorithm for managing residential distributed energy resources, IEEE Trans. Smart Grid 5 (2014) 2360–2367, https://doi.org/10.1109/TSG.2014.2325912.

[14] M.J. Sanjari, H. Karami, A.H. Yatim, G.B. Gharehpetian, Application of Hyper-Spherical Search algorithm for optimal energy resources dispatch in residential microgrids, Appl. Soft Comput. 37 (2015) 15–23, https://doi.org/10.1016/j.asoc.2015.08.006.

[15] H. Ren, W. Gao, Y. Ruan, Optimal sizing for residential CHP system, Appl. Therm. Eng. 28 (2008) 514–523, https://doi.org/10.1016/j.applthermaleng.2007.05.001.

[16] Y. Yang, W. Pei, Z. Qi, Optimal sizing of renewable energy and CHP hybrid energy microgrid system, 2012 IEEE Innov Smart Grid Technol - Asia, ISGT Asia (2012) (2012) 1–5, https://doi.org/10.1109/ISGT-Asia.2012.6303122.

[17] C. Brandoni, M. Renzi, Optimal sizing of hybrid solar micro-CHP systems for the household sector, Appl. Therm. Eng. 75 (2015) 896–907, https://doi.org/10.1016/j.applthermaleng.2014.10.023.

[18] M.H. Moradi, M. Eskandari, S. Mahdi Hosseinian, Operational strategy optimization in an optimal sized smart microgrid, IEEE Trans. Smart Grid 6 (2015) 1087–1095, https://doi.org/10.1109/TSG.2014.2349795.

[19] B. Aluisio, M. Dicorato, G. Forte, M. Trovato, An optimization procedure for Microgrid day-ahead operation in the presence of CHP facilities, Sustain. Energy. Grids Networks 11 (2017) 34–45, https://doi.org/10.1016/J.SEGAN.2017.07.003.

[20] M. Sharafi, T.Y. ElMekkawy, E.L. Bibeau, Optimal design of hybrid renewable energy systems in buildings with low to high renewable energy ratio, Renew. Energy 83 (2015) 1026–1042, https://doi.org/10.1016/J.RENENE.2015.05.022.

[21] W.G.J. Van Helden, R.J.C. Van Zolingen, H.A. Zondag, PV Thermal systems: PV panels supplying renewable electricity and heat, Prog. Photovoltaics Res. Appl. 12 (2004) 415–426, https://doi.org/10.1002/pip.559.

[22] T.N. Anderson, M. Duke, G.L. Morrison, J.K. Carson, Performance of a building integrated photovoltaic/thermal (BIPVT) solar collector, Sol. Energy 83 (2009) 445–455, https://doi.org/10.1016/j.solener.2008.08.013.

[23] C. Renno, Optimization of a concentrating photovoltaic thermal (CPV/T) system used for a domestic application, Appl. Therm. Eng. 67 (2014) 396–408, https://doi.org/10.1016/j.applthermaleng.2014.03.026.

[24] S. Singh, S. Agrawal, R. Gadh, Optimization of single channel glazed photovoltaic thermal (PVT) array using Evolutionary Algorithm (EA) and carbon credit earned by the optimized array, Energy Convers. OR Manag. 105 (2015) 303–312, https://doi.org/10.1016/j.enconman.2015.07.062.

[25] M.I. Hussain, G.H. Lee, Parametric performance analysis of a concentrated photovoltaic co-generation system equipped with a thermal storage tank, Energy Convers. Manag. 92 (2015) 215–222, https://doi.org/10.1016/j.enconman.2014.12.054.

[26] H. Gholami, A. Khalilnejad, G.B. Gharehpetian, Electrothermal performance and environmental effects of optimal photovoltaic-thermal system, Energy Convers. Manag. 95 (2015) 326–333, https://doi.org/10.1016/j.enconman.2015.02.014.

[27] M.H. Balali, N. Nouri, E. Omrani, A. Nasiri, W. Otieno, An overview of the environmental, economic, and material developments of the solar and wind sources coupled with the energy storage systems, Int. J. Energy Res (2017), https://doi.org/10.1002/er.3755.

[28] A. Lorestani, M.M. Ardehali, G.B. Gharehpetian, Optimal resource planning of smart home energy system under dynamic pricing based on invasive weed optimization algorithm, in: 2016 Smart Grids Conf, IEEE, 2016, pp. 1–8, https://doi.org/10.1109/SGC.2016.7883462.

[29] H. Gharavi, M.M. Ardehali, S. Ghanbari-Tichi, Imperial competitive algorithm optimization of fuzzy multi-objective design of a hybrid green power system with considerations for economics, reliability, and environmental emissions, Renew. Energy 78 (2015) 427–437, https://doi.org/10.1016/j.renene.2015.01.029.

[30] B. Arandian, M.M. Ardehali, Effects of environmental emissions on optimal combination and allocation of renewable and non-renewable CHP technologies in heat and electricity distribution networks based on improved particle swarm optimization algorithm, Energy 140 (2017) 466–480, https://doi.org/10.1016/j.energy.2017.08.101.

[31] T. Niknam, M.R. Narimani, J. Aghaei, R. Azizipanah-Abarghooee, Improved particle swarm optimisation for multi-objective optimal power flow considering the cost, loss, emission and voltage stability index, Gener. Trans. Distrib. IET 6 (6) (2012) 515, https://doi.org/10.1049/iet-gtd.2011.0851.

[32] L. Kujanpää, E. Pursiheimo, Techno-economic evaluation of flexible CCS concepts in a CHP system, Energy Procedia 114 (2017) 6638–6649, https://doi.org/10.1016/j.egypro.2017.03.1818.

Nomenclature

A: Area of PV and collector (m^2)
AD: Number of autonomy day
b_{rand}: A random integer number
C: Cost
C_1: Cognitive weight
C_2: Social weight
Cs: Capacity of storage unit (kWh)
CR: Crossover rate
DM: Dimensional search space
DOD: Depth of discharge
E: Electrical power (kW)
En: Daily load energy (kWh)
f: Fitness value
fGbest: Fitness value of the global best
F: Random positive parameter
F_R: Heat removal efficiency
G: Solar irradiation (kW/m^2)
Gbest: Global best position
h: Anemometer height
i: Interest rate
it: Number of iteration
j: Number of particle
K: Shape-shift coefficient
LPS: Loss of power supply
LPSP: Loss of power supply probability
M: Mutant vector
MaxIt: Maximum number of iteration
n: Life of RE-CHP system (year)
n′: Life of equipment (year)
N: Number of elements
NOCT: Cell nominal operating temperature
nPop: Number of population
Pbest: Personal best position
Pr: Price per unit of component ($)
SOC: Stored energy in storage system (kWh)
T: Temperature (k)
TC: Total cost ($)
Th: Thermal power (kW)
U_{loss}: Heat loss coefficient (W/m^2K)
X: Position Vector
V: Velocity

Greek symbols

α: Friction coefficient of the landscape
β: Temperature coefficient (K^{-1})
ε: Heat loss coefficient (h^{-1})
η: Efficiency

σ: Hourly self-discharge rate of the battery
τ: Specified period
τα: Transmission and absorption coefficient
ω: Inertia weight

Subscripts

a: Ambient
Conv/Inv: Converter or inverter
Cap: Capital
CRF: Capital recovery factor
Cut-in: Cut-in speed of wind turbine
Cut-out: Cut-out speed of wind turbine
dump: Dumped energy
E: Electrical
EES: Electrical energy storage
EH: Electrical heater
f: Fluid (water)
h: Heat use efficiency
inv: Inverter
Load: Load
O&M: Operation and maintenance
PV: Photovoltaic
PVT: Photovoltaic-thermal
r: Rated
ref: Reference
Rand: Uniform distributed random numbers
TES: Thermal energy storage
Th: Thermal
w: Wind
WT: Wind turbine

Superscripts

Min: Minimum
Max: Maximum
t: Time interval
P: Present Worth

Acronyms

RE: Renewable energy
CHP: Combined heat and power
CRF: Capital recovery factor
CS: Cuckoo search
DE: Differential evolution
EH: Electrical heater
EMS: Energy management controller
EES: Electrical energy storage
E-PSO: Evolutionary particle swarm optimization
FC: Fuel cell
GA: Genetic algorithm
HSA: Harmony search algorithm
HSS: Hyper-spherical search algorithm
ICA: Imperialistic competition algorithm
LMM: Levenberge Marquardt method
LP: Linear programming
LPSP: Loss of power supply probability
MINP: Mixed integer nonlinear Programming
MT: Micro-turbine
NG: Natural gas
OV: Optimization variable
PV: Photovoltaic
PVT: Photovoltaic-thermal
QP: Quadratic Programming
SA: Simulated Annealing
SQP: Sequential quadratic programing
TAC: Total annual cost
TES: Thermal energy storage
WT: Wind turbine